UCSF
UC San Francisco Previously Published Works

Title
Molecular requirements for actin-based lamella formation in Drosophila S2 cells.

Permalink
https://escholarship.org/uc/item/2wd001k6

Journal
The Journal of cell biology, 162(6)

ISSN
0021-9525

Authors
Rogers, Stephen L
Wiedemann, Ursula
Stuurman, Nico
et al.

Publication Date
2003-09-01

DOI
10.1083/jcb.200303023

Peer reviewed

eScholarship.org Powered by the California Digital Library
University of California

JCB Article

Molecular requirements for actin-based lamella formation in *Drosophila* S2 cells

Stephen L. Rogers, Ursula Wiedemann, Nico Stuurman, and Ronald D. Vale

Howard Hughes Medical Institute and Department of Cellular and Molecular Pharmacology, University of California, San Francisco, San Francisco, CA 94107

Cell migration occurs through the protrusion of the actin-enriched lamella. Here, we investigated the effects of RNAi depletion of ~90 proteins implicated in actin function on lamella formation in *Drosophila* S2 cells. Similar to in vitro reconstitution studies of actin-based *Listeria* movement, we find that lamellae formation requires a relatively small set of proteins that participate in actin nucleation (Arp2/3 and SCAR), barbed end capping (capping protein), filament depolymerization (cofilin and Aip1), and actin monomer binding (profilin and cyclase-associated protein). Lamellae are initiated by parallel and partially redundant signaling pathways involving Rac GTPases and the adaptor protein Nck, which stimulate SCAR, an Arp2/3 activator. We also show that RNAi of three proteins (kette, Abi, and Sra-1) known to copurify with and inhibit SCAR in vitro leads to SCAR degradation, revealing a novel function of this protein complex in SCAR stability. Our results have identified an essential set of proteins involved in actin dynamics during lamella formation in *Drosophila* S2 cells.

Introduction

Cell motility is essential for the precise spatial and temporal orchestration of tissue morphogenesis that gives rise to the elaborate, three-dimensional architecture of an organism. Cellular migration remains crucial throughout the lifetime of higher organisms, enabling processes such as wound healing and chemotactic responses in the immune system. Metastasis demonstrates a more sinister manifestation of cell motility in which transformed cells relocate from a primary tumor and colonize a secondary site.

Cell migration can be subdivided into three stages (Lauffenburger and Horwitz, 1996; Mitchison and Cramer, 1996). The first stage is protrusion of the leading edge, the polarized "front" of the cell. During protrusion, the cell fabricates a dense, actin-rich structure called the lamella, which extends the leading edge in the direction of migration (Small et al., 2002). The second stage involves adhesion of the advancing leading edge to the substrate. This complex process involves extracellular adhesion receptors forming transmembrane linkages between the extracellular matrix and the actin cytoskeleton. These attachment sites mature to become focal adhesions, structures that allow the cell to exert force upon its surroundings by contraction of its actin cytoskeleton. In the third stage, the trailing edge releases from the extracellular matrix and is retracted toward the front of the cell. This process involves dissolution of adhesion structures and contraction of the cytoskeleton by actomyosin to "pull" the rear of the cell forward. In this study, we focused on the first of these stages: the actin-based protrusive forces that give rise to lamellae.

The dynamics of the actin cytoskeleton that underlie the propulsive forces at the leading edge have been extensively investigated, and the information has been synthesized into the dendritic nucleation/treadmilling model (Pollard et al., 2000; Pollard and Borisy, 2003). According to this model, new actin filaments are nucleated by the Arp2/3 complex and grow in a polarized fashion with the fast-growing barbed ends oriented toward the leading edge. The new filaments are nucleated from Arp2/3 bound to the sides of preexisting filaments, giving rise to the branched dendritic array of filaments observed by electron microscopy (Welch and Mullins, 2002). Arp2/3 is normally repressed, but can be activated by the WASP and SCAR family of proteins, which in turn are activated though small G proteins (e.g., Rac and Cdc42) that are integrated into many signaling cascades (Etienne-Manneville and Hall, 2002). The collective force of individual actin filaments polymerizing at the leading

The online version of this article includes supplemental material.

Address correspondence to Ron Vale, Department of Cellular and Molecular Pharmacology, University of California, San Francisco, N312 Genentech Hall, 600 16th Street, San Francisco, CA 94107. Tel.: (415) 476-6380. Fax: (415) 476-5233. email: vale@phy.ucsf.edu

Key words: actin; lamella; polymerization; SCAR; cytokinesis

Abbreviations used in this paper: CAP, cyclase-associated protein; con A, concanavalin A; VASP, vasodilator-stimulated phosphoprotein.

© The Rockefeller University Press, 0021-9525/2003/09/1079/10 $8.00

edge is thought to push the membrane forward (Mogilner and Oster, 1996). This pushing force is attenuated by blocking further monomer addition to barbed ends by capping protein (Cooper and Schafer, 2000) and by the rearward "retrograde flow" of the actin filament lattice as a whole (Cramer, 1997). The activity of capping protein can be antagonized by the enabled/Mena/vasodilator-stimulated phosphoprotein (VASP) family, which thereby acts to promote leading edge formation (Bear et al., 2002). Toward the rear of the lamella, actin filaments become debranched, severed, and depolymerized by cofilin-like proteins, and the released monomeric actin is recycled into polymer at the leading edge. In addition to lamella, many cells form elongate and narrow actin projections called filopodia (Small et al., 2002). Many actin-binding proteins have been described in these structures, but the mechanism of filopodia formation is poorly understood compared with lamella formation.

The roles and activities of the actin-interacting proteins described above (as well as many others) have been elucidated primarily using in vitro assays for actin assembly (Pollard and Borisy, 2003). The yeast *Saccharomyces cerevisiae* also has been a powerful system for investigating the roles of actin-binding proteins in vivo (Ayscough and Drubin, 1996), although the actin architecture in yeast differs considerably from the lamella and filopodia found in higher eukaryotes. In addition, mutations in many actin-binding proteins have been described in *Drosophila* and *Caenorhabditis elegans* (Montell, 1999). However, not all of these are null mutations, and the analyses in the literature have been performed on various cell types in embryos or mature animals. Here, we have investigated the in vivo roles of ~90 actin-binding proteins in a single cell type, the *Drosophila* S2 cell line for which we have developed conditions for observing lamella formation and dynamics.

Results

Drosophila S2 cells spread and form an actin-rich lamella on concanavalin A–coated surfaces

Under routine culture conditions, S2 cells display a roughly spherical morphology with a diameter of ~10 μm (Fig. 1, a and b). These cells are not motile and exhibit no obvious morphological polarity, but time-lapse microscopy of cells expressing GFP–actin revealed that their surfaces are dynamic and continuously extend and absorb membrane ruffles (Video 1, available at http://www.jcb.org/cgi/content/full/jcb.200303023/DC1). S2 cells may be induced to undergo a dramatic change in their morphology when plated on glass coverslips coated with the lectin concanavalin A (con A) (Rogers et al., 2002). Within 20 to 30 min after plating on this substrate, these cells avidly attach, flatten, and spread to adopt a discoid morphology of approximately double their normal diameter (20 μm). Spread cells resemble a "fried egg" with a domed central region containing the nuclei and majority of organelles surrounded by a thin, organelle-free zone (Fig. 1, c and d; Video 2, available at http://www.jcb.org/cgi/content/full/jcb.200303023/DC1).

To better understand the organization of actin in S2 cells, we fixed con A–adhered S2 cells expressing GFP–actin or stained them with Texas red X-phalloidin, a probe that selectively binds to filamentous actin. When examined by fluorescence microscopy, most S2 cells (90%) exhibited a highly developed, radially symmetrical actin cytoskeleton that could be divided into three zones: a dense peripheral network at the extreme periphery of the cells (~1 μm wide), a second central zone (4–6 μm wide) of lower actin density composed of filaments, and a third circular bundle of filaments that surrounded the nucleus (Fig. 2, a and b). Arp3, cofilin, and capping protein were enriched in this first actin-dense zone at the leading edge, especially at membrane ruffles (Fig. 2, a, c, and f). Enabled/VASP was further restricted to the extreme edge of the periphery (<1 μm) (Fig. 2 e). In contrast, immunolocalization of profilin/chickadee revealed puncta that were distributed throughout the cell and particularly abundant in the inner nuclear and organelle-rich do-

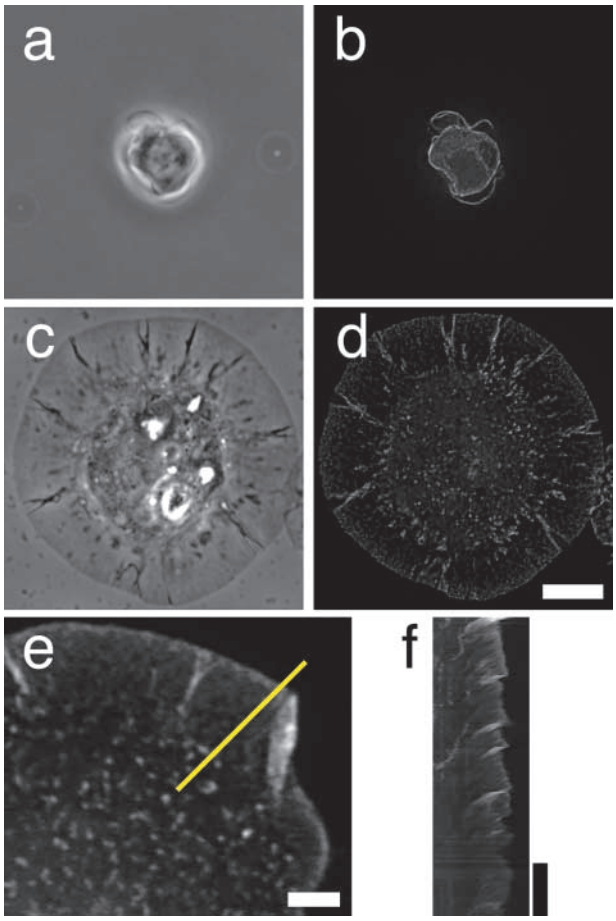

Figure 1. ***Drosophila* S2 cells attach, spread, and form lamellae when plated on con A.** S2 cells expressing EGFP–actin were plated on polylysine (a and b) or con A (c and d) and examined by phase contrast (a and c) or fluorescence microscopy (b and d). Cells on polylysine retain a spherical morphology but form actin-containing membrane ruffles along their surface. When plated on con A, the majority of S2 cells (>90%) spread to form a radially symmetrical actin-based lamellae (c and d). Bar, 5 μm. (e) A single frame from a time-lapse movie of an S2 cell expressing GFP–actin and plated on con A. The yellow line represents the region of the movie used to generate the kymograph shown in f. Bar, 1 μm. (f) This kymograph shows the behavior of actin over time in a lamella. The shark fin shape is indicative of cycles of extension and retraction at the cell margin, while the diagonal lines visualize the retrograde flow of actin at the cell periphery. Bar, 30 s.

The Journal of Cell Biology

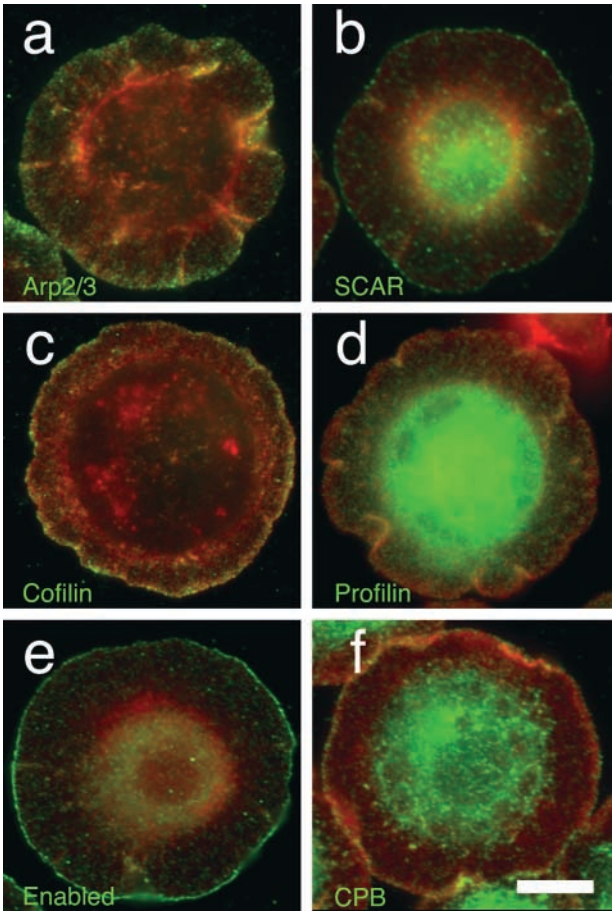

Figure 2. **Immunofluorescence localization of actin regulatory proteins to lamellae of S2 cells.** S2 cells were plated on con A for 1 h and then fixed and double stained for actin (red) and Arp3 (a, green), SCAR (b, green), cofilin/twinstar (c, green), profilin (d, green), enabled (e, green), or capping protein (f, green). Bar, 5 μm.

main (Fig. 2 d). These puncta were not associated with adhesion structures, as immunofluorescent staining against phosphotyrosine failed to stain the ventral surface of the cells (unpublished data). The distributions of these well-characterized actin-binding proteins are generally similar to those described in other cell types that form actin-rich lamellae.

A small proportion (<10%) of cells did not exhibit such well-spread lamella but rather possessed numerous and dynamic filopodia evenly spaced around their circumference (Fig. S1, available at http://www.jcb.org/cgi/content/full/jcb.200303023/DC1). These short (1–2 μm) projections exhibited cycles of elongation and retraction (Video 3, available at http://www.jcb.org/cgi/content/full/jcb.200303023/DC1). We have not observed interconversion of the two cell morphologies. We restricted our RNAi studies to the predominant population of cells that spread and form lamella on the con A–coated surfaces.

We also directly visualized actin dynamics in the lamellae of living S2 cells expressing GFP–actin after plating on con A. Membrane ruffles formed at the cell periphery, folded back toward the cell center, and ultimately fused with the dorsal surface of the cell (Video 4, available at http://www.jcb.org/cgi/content/full/jcb.200303023/DC1). Such ruffling activity was more or less symmetrically distributed around the cell, and we rarely observed polarized morphologies or cell movement. At sufficiently low levels of protein induction, a speckled pattern of GFP–actin (Waterman-Storer et al., 1998) was observed, and time-lapse imaging revealed a centripetal flow of actin from the periphery toward the center of the cell at a rate of ~4.0 ± 0.44 μm/min (Fig. 1, e and f), which is somewhat faster than described in other systems, such as migrating fibroblasts or neuronal growth cones (Cramer, 1997). In summary, our imaging of actin and actin-binding proteins indicates that con A–induced spreading of S2 cells constitutes an attractive model system for understanding the molecular basis of lamella formation.

Protein requirements for lamella formation

To dissect the molecular basis of lamella formation, we exploited the susceptibility of S2 cells to RNAi to identify proteins involved in this process. We compiled a candidate list of ~90 proteins implicated in aspects of actin function or in cell motility during neuronal development and dorsal closure during *Drosophila* embryogenesis (Table I).

DNA microarray analysis demonstrated that only five genes in this list are not expressed above background levels in S2 cells (Table I; Hollien, J., and J. Weissman, personal communication). As very low expressing genes nevertheless may be important for cell function, we still subjected these genes to RNAi analysis. A 7-d RNAi treatment was used to deplete proteins before assaying the cells for lamella formation on con A–treated coverslips. Filamentous actin was visualized with rhodamine-phalloidin, and DNA was stained with DAPI to screen for multiple nuclei reflecting cytokinesis defects. For every treatment, we examined at least 500 cells. We verified the efficacy of our RNAi treatments by immunoblotting extracts from dsRNA-treated cells using a panel of antibodies to 13 proteins to which we had access (Fig. 3 i). Immunoblotting for those tested revealed that RNAi reduced protein expression by at least 90% of endogenous levels and in many cases was not detectable. This immunoblot analysis included five proteins for which RNAi did not elicit an obvious phenotype (Table I). In the accompanying paper (Goshima and Vale, 2003), we also demonstrate >90% reduction in the levels of 10 motor proteins subjected to RNAi and have yet to encounter a case where RNAi has failed to reduce protein levels. We, therefore, speculate that dsRNAs against proteins that we could not quantitate most likely produced a similar degree of inhibition.

Of the ~90 genes tested, we found that RNAi produced obvious aberrant morphologies in 19 cases (Table I; all RNAi experiments were performed at least twice). The observed defects can be categorized into seven phenotypic classes that will be described below.

Class 1: p20 subunit of Arp2/3, SCAR, kette, Abi, and Sra-1

We inactivated the Arp2/3 complex by targeting its crucial p20 subunit, which mediates protein–protein interactions within the Arp 2/3 complex and, therefore, is essential for stability and actin-nucleating activity (Gournier et al., 2001). After p20 RNAi, >90% of S2 cells exhibited a striking mor-

Table I. **Morphological classification for RNAi treatments in this study**

Class 1: stellate morphology			
p20 subunit of Arp2/3	SCAR[a]	kette	Nck/dreadlocks[a]
Sra-1	Abi		
Class 2: failure to spread and filamentous actin accumulation at cortex			
cofilin/twinstar[a]	Aip1		
Class 3: Failure to spread and filamentous actin throughout cell			
profilin/chickadee[a]	CAP/act up		
Class 4: increased width of lamellae			
slingshot			
Class 5: increased membrane ruffling			
capping protein β[a]			
Class 6: formation of thin processes			
Cdc42			
Class 7: cytokinesis failure			
myosin II/zipper	profilin/chickadee[a]	cofilin/twinstar[a]	anillin
citron kinase	Rho1[a]	CAP/act up	Aip1
diaphanous[a]	AcGAP		
No effect on lamellae			
Abl kinase	enabled	myosin IA	Rab5
Adf/cofilin-like	fascin[a]	myosin IB	Rac1/2
basket	filamin	myosin V	RhoBTB
cappucino	fimbrin	myosin VI[a]	RhoL
ciboulot	forked[b]	myosin VII	rhophilin
coracle	formin/DIA-like	myosin VII (28B)	sanpodo
coronin	gelsolin	myosin XV	spire[b]
cortactin	Genghis Kahn	myosin XVIII (PDZ)	talin
Cdk5	hemipterous	Nck (dreadlocks)[a]	Trio
Dab (disabled)	kelch	nullo	tropomyosin I
Dah	Lgl[a]	ovarian tumor	tropomyosin II
dcarmil	Lim kinase	Pak1 kinase	twinfillin
DLAR[b]	merlin	protein kinase N	Vav
drebin-like	moesin	POD-1/coronin[a]	villin-like
Drk	Mtl (Rac-like)	Pp2A	vinculin
DROK	mushroom bodies tiny	quail[b]	WASP
E-cadherin (shotgun)	myoblast city[b]		

For complete gene information, see the online supplemental material (available at http://www.jcb.org/cgi/content/full/jcb.200303023/DC1). Depletion of myosin II/zipper also caused impaired lamella spreading and actin disorganization. Inhibition of Rac1/2 also generated an increase in stellate phenotypes in combination with Nck (see Fig. 4).

[a]Protein reduction confirmed by immunoblot analysis.

[b]Expression levels of these genes by Affymetrix DNA microarray analysis was not detected above background levels in S2 cells (Hollien, J., and J. Weissman, personal communication). The following genes were not evaluated by microarray analysis: gelsolin, myosin XVIII, nullo, Pp2A, and tropomyosin II. All other genes are expressed in S2 cells.

phological defect when plated on con A. Instead of the circular, symmetrical shape usually induced on this substrate, p20-depleted cells adopted a stellate, radially asymmetrical cell morphology (Fig. 3 a). Phalloidin staining revealed that these cells rarely formed lamellae; instead filamentous actin was enriched in the distal tips of a variable number of tapered projections. The presence of actin filaments could be due to residual Arp2/3 or to alternative actin-nucleating activities. In addition, actin filaments were sometimes observed to run radially from the center of the cell body along the lengths of these projections. These processes were also enriched in microtubules that often extended to their distal regions (unpublished data). The frequency of multinucleate cells was approximately the same as control cells, indicating that inhibition of Arp2/3 did not affect cytokinesis.

Cells contain actin nucleation–promoting factors that activate the Arp2/3 complex (Welch and Mullins, 2002). Genetic analysis in *Drosophila* has shown that one of these factors, SCAR, is essential for numerous actin-based processes during development, while WASP, another activator, mediates a subset of Arp2/3 functions in neuronal cell fate determination (Ben-Yaacov et al., 2001; Zallen et al., 2002). WASP RNAi did not alter cell morphology or actin organization in S2 cells. In contrast, we found that RNAi against SCAR exactly duplicated the morphological defects observed with RNAi of the p20 subunit of Arp2/3 in >80% of the cells (unpublished data). Interestingly, RNAi for three proteins (kette, Sra-1, and Abi) that were recently identified to copurify with SCAR (Eden et al., 2002) produced a phenotype indistinguishable from

The Journal of Cell Biology

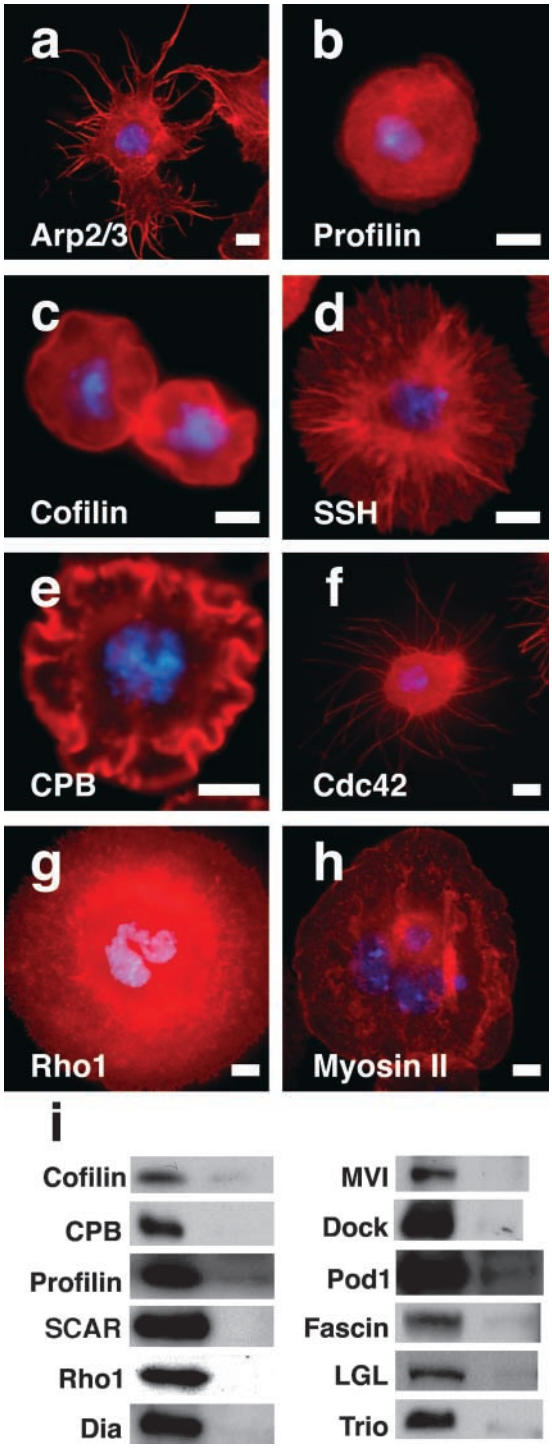

Figure 3. **RNAi-mediated inhibition of actin regulatory proteins disrupts normal cellular morphology in S2 cells on con A.** Untreated cells are shown in Fig. 1 (c and d). Cells were treated with dsRNA against the p20 subunit of the Arp2/3 complex (a), profilin/chickadee (b), cofilin/twinstar (c), slingshot (d), capping protein β (e), Cdc42 (f), Rho1 (g), and myosin II/zipper (h) for 7 d and then plated on con A and stained with rhodamine-phalloidin (red) and DAPI (blue) to visualize filamentous actin and DNA, respectively. (i) Immunoblots demonstrating the effectiveness of RNAi on the levels of 13 different proteins: cofilin/twinstar, capping protein β (CPB), SCAR, Rho1, diaphanous (Dia), enabled (Ena), myosin VI (MVI), Nck/dreadlocks (Dock), Pod1, fascin/singed, lethal giant larvae (LGL), and Trio. Exactly 10 μg of total cellular protein was loaded for each lane. Bars, 5 μm.

SCAR or p20. The role of these subunits will be described in more detail in a subsequent section. Thus, we conclude that lamella formation in S2 cells is a SCAR–Arp2/3-dependent process.

Class 2: profilin and cyclase-associated protein

The second category of RNAi-induced morphological defect was typified by inhibition of profilin, an actin monomer–binding protein (Cooley et al., 1992). After this treatment, >85% of cells failed to spread on con A and instead retained their spherical shape (Fig. 3 b). Phalloidin staining was diffuse throughout these cells, however, individual filaments could not be resolved. These cells also were defective in cytokinesis, as revealed by the high incidence of multiple nuclei (39%, $n = 846$), which is consistent with prior studies (Verheyen and Cooley, 1994). A similar morphology also was generated by RNAi against cyclase-associated protein (CAP/act up), another monomeric actin–binding protein that has been shown to play an important role in actin organization in *Drosophila* (Baum et al., 2000; Benlali et al., 2000). When bound to monomeric actin, profilin acts to restrict actin incorporation to the barbed-end of actin filaments and mediates exchange of ADP for ATP (Holt and Koffer, 2001). We speculate that the accumulation of f-actin in profilin and CAP RNAi cells, along with the failure to form lamellae, may reflect nonproductive polymerization of actin filaments from both the barbed and pointed ends.

Class 3: cofilin and Aip1

The actin-binding protein cofilin/twinstar is essential for actin-based functions in many cell types, and in vitro and in vivo studies indicate a role for cofilin in actin filament severing and turnover (Gunsalus et al., 1995). Inhibition of cofilin by RNAi prevented S2 cell spreading on con A in >95% of treated cells. These cells retained their spherical morphology, and phalloidin staining revealed a dramatic cortical accumulation of filamentous actin as well as a wrinkled "raisin-like" texture to the surface of the cell (Fig. 3 c). The abnormal accumulation of filamentous actin within the cells suggests that actin turnover is inhibited in S2 cells depleted of either of these two proteins. Cofilin-inhibited S2 cells exhibited a high incidence of multinucleate cells, implicating a role in cytokinesis (24.6%, $n = 645$), as previously demonstrated (Gunsalus et al., 1995). This morphology and actin distribution was mimicked by RNAi inhibition of Aip1, a protein that acts cooperatively with cofilin in disassembling actin in *Xenopus* and budding yeast (Okada et al., 1999; Rodal et al., 1999). Aip1 also produced a cytokinesis defect (unpublished data). These results indicate that both cofilin and Aip1 are essential for actin remodeling during lamella formation and that, despite the similarities in cell morphology produced by RNAi against either of them, these two proteins have distinct roles in actin regulation.

Class 4: slingshot

Slingshot is a protein phosphatase that activates the actin-severing activity of cofilin; loss-of-function experiments in

Drosophila have demonstrated that tissues mutant for slingshot exhibit abnormal accumulations of f-actin (Niwa et al., 2002). S2 cells treated with dsRNA to inhibit slingshot were able to attach and spread efficiently on con A. However, the lamellae in >50% of these cells exhibited structural abnormalities as compared with controls. The distribution of f-actin was uniformly dense from the cell periphery to the center of the cell and did not show the typical distal enrichment commonly observed in spread S2 cells (Fig. 1 d). Cells exhibiting this morphology typically had prominent radial bundles of actin that spanned the entire width of the lamellae. We speculate that this cellular morphology is produced by a partial loss of cofilin activity, leading to inefficient disassembly of the dendritic array of actin filaments at the rear of the lamellae and thus producing a lamellipod that is radially wider than normal. Cytokinesis defects were not observed in these cells.

Class 5: capping protein

Capping protein is an important regulatory factor that binds to the barbed ends of actin filaments to prevent actin monomer addition (Cooper and Schafer, 2000). Recent studies have suggested that a functional antagonism between capping protein and enabled/VASP regulates the length and polymerization rate of actin filaments in the lamella (Bear et al., 2002). This balance controls the rate of lamella protrusion in motile cells. S2 cells treated with dsRNA against capping protein adhered and spread normally, but ~80% had lamellae exhibiting a hyper-ruffled shape (Fig. 2 f). Lamellae in S2 cells lacking capping protein also exhibited an accumulation of filamentous actin at the periphery that extended 2–3 μm inwards from the cell perimeter, as compared with ~1 μm in untreated cells (Fig. 3 e). The results of Bear et al. (2002) suggest an explanation for the abnormal lamella morphology. In the absence of capping protein, enabled/VASP-mediated actin filament elongation favors the formation of abnormally long filaments at the cell margin. These filaments push against the membrane, fueling protrusion, until compressive forces exceed the flexural rigidity of long filaments, causing them to buckle and the membrane to retract. This hypothesis explains the hyper-ruffled phenotype as well as the accumulation of f-actin at the margin of the cell. We did not observe an accumulation of multinucleated cells, suggesting that capping protein is dispensable for cytokinesis.

Class 6: Cdc42

A sixth category of morphological defect was produced by depletion of Cdc42 by RNAi. Cdc42, a member of the Rho family of small G proteins, regulates actin organization and is generally thought to mediate the formation of filopodia during cellular migration (Etienne-Manneville and Hall, 2002). Inhibition of Cdc42 prevented formation of a normal lamella in ~50% of the cells. Instead, actin was organized into long, thin processes that projected from the entire periphery of the cell (Fig. 3 f). These processes did not resemble the filopodia that spontaneously form on some S2 cells or that form in response to overexpression of constitutively active Cdc42V12 (unpublished data), because they were typically >10 μm in length and possessed a uniform diameter. This morphology is difficult to reconcile with what is known about Cdc42 functions, although a cellular null phenotype for Cdc42 in metazoan cells has not been reported to our knowledge. This phenotype will be investigated more closely in a further study.

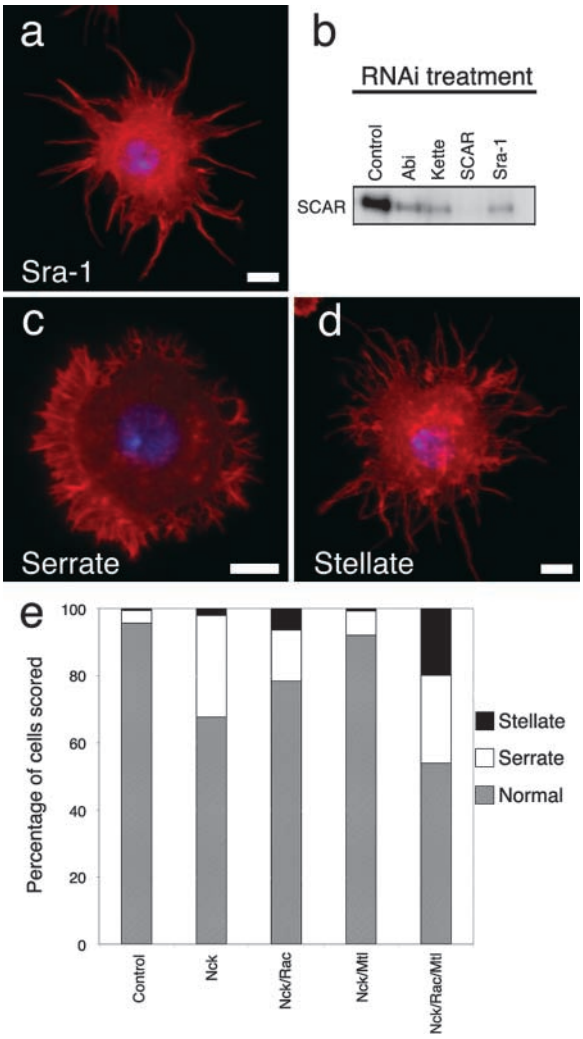

Figure 4. **Control of SCAR degradation and activation.** Inhibition of SCAR-associated proteins kette, Sra-1, or Abi by RNAi causes degradation of SCAR itself. S2 cells were treated with dsRNA corresponding to the coding sequence for Sra-1 (a) for 7 d and then plated on con A and stained with phalloidin to visualize actin (red) and DAPI to view DNA (blue). The morphology of these cells closely resembles the defects in lamellae formation produced by Arp2/3 and SCAR RNAi (Fig. 3, b and c). Similar results were observed with RNAi against kette and Abi (not depicted). Bar, 5 μm. (b) Quantitative immunoblotting of cells treated with dsRNA versus Abi, kette, SCAR, and Sra-1 with antibodies against SCAR. Depletion of these proteins by RNAi decreases the amount of SCAR present in S2 cells. Equal protein loading was verified by Bradford assay (not depicted). (c and d) Cells treated with dsRNAi to simultaneously inhibit Rac1, Rac2, Mtl, and Nck show a variety of lamella defects. Among these are a malformed, serrate cell margin (c) and the stellate morphology similar to SCAR RNAi (Fig. 3, b and c). (e) Graph showing the quantitation of morphological defects caused by inhibition of Nck, Rac1/2, and Mtl. Bars, 5 μm.

Table II. **Effects of Rac1, Rac2, Mtl, and Nck RNAi on cell morphologies**

Morphology	Control (814)	Nck (550)	Nck + Rac1/2 (616)	Nck + Mtl (580)	Nck + Rac1/2 + Mtl (570)
	%	%	%	%	%
Normal	95.5	67	78.2	91.8	53.6
Serrate	3.8	30	15.2	7.3	26
Stellate	0.6	2.1	6.4	0.7	19.8

Classifications are represented as percentages of the total number of cells observed (in parentheses).

Class 7: myosin II, Rho1, AcGAP, diaphanous, citron kinase, anillin, scraps, and Rho1

A seventh category was failure of cytokinesis without inhibition of cell spreading on con A–coated surfaces (Fig. 3 g). Cells in this category (>95%) possessed multiple nuclei and were much larger in diameter than control cells. Phalloidin staining revealed that, despite their larger size, cells were able to form lamellae with normal architecture. Inhibition of Rho1 and its downstream effectors citron kinase, diaphanous, AcGAP, and myosin II typified this defect. Many of these molecules were recently identified in a similar S2-based RNAi screen for genes specifically involved in cytokinesis, but Aip1, CAP, citron kinase, and diaphanous were not tested in this study (Somma et al., 2002).

In addition to producing cytokinesis defects, however, cells depleted of cytoplasmic myosin II sometimes (48.6%, $n = 768$) failed to form normal lamellae, in addition to producing cytokinesis defects (Fig. 3 h). These cells contained abundant filamentous actin, as judged by phalloidin staining, but the actin cytoskeleton displayed an overall lack of organization with filaments criss-crossing the width of the cell in an apparently random manner. These results reveal a role for myosin II in the organization of actin in the lamellae.

The SCAR-associated proteins kette, Sra-1, and Abi prevent degradation of SCAR

The recent biochemical study by Eden et al. (2002) demonstrated that native SCAR exists in a trans-inhibited state in a complex with the kette, Sra-1, and Abi proteins. Given the demonstrated role of these proteins in suppressing SCAR activity in vitro, we were surprised that RNAi-mediated depletion of Sra-1 (Fig. 4 a), Abi, or kette resulted in a SCAR-like phenotype rather than in excessive actin polymerization. One hypothesis to account for these observations was that SCAR was either not localized at the membrane or degraded in the absence of members of the kette–Sra-1–Abi complex. To test these ideas, we stained kette, Abi, or Sra-1 RNAi–treated cells with anti-SCAR antibodies and observed that the overall staining intensities were reduced or eliminated (unpublished data). We next performed quantitative immunoblotting and found that kette, Sra-1, and Abi RNAi treatments caused a considerable reduction of SCAR levels in S2 cells (Fig. 4 b). Depletion of Abi, kette, and Sra-1 reduced SCAR protein levels to 34.3 ± 18, 17.3 ± 9.5, and 9.6 ± 2.6%, respectively ($n = 3$). In contrast, cells treated with dsRNA versus diaphanous did not show reduced SCAR levels (unpublished data). From these observations, we conclude that the kette–Sra-1–Abi complex is required for SCAR stability.

The small G proteins Rac1/2 and Mtl and the adaptor protein Nck mediate cell spreading and lamella formation via two independent pathways

Activation of SCAR proteins is generally thought to be mediated by Rac GTPases (Welch and Mullins, 2002). However, RNAi of *Drosophila* Rac 1, Rac 2, and the Rac-like protein Mtl (Hakeda-Suzuki et al., 2002) did not prevent cell spreading or lamella formation (Table II). Genetic evidence has demonstrated that these small G proteins are functionally redundant in many tissues in the fly (Hakeda-Suzuki et al., 2002). Furthermore, in vitro experiments showed that the inhibitory SCAR complex could be activated either by Rac1 or the SH2-SH3 adaptor protein Nck (Eden et al., 2002). To test whether this was the case in S2 cells, we treated cells with dsRNA designed to simultaneously inhibit Rac1 and Rac2 (Rac1/2) and Mtl for 7 d. Unexpectedly, phalloidin staining revealed that these dsRNA-treated cells spread and formed a normal lamella when plated on con A (unpublished data).

We then tested the in vitro finding of Eden et al. (2002) that either Rac or Nck is able to activate SCAR by simultaneously inhibiting various combinations of Rac1/2, Mtl, and the *Drosophila* orthologue of Nck (dreadlocks). This treatment produced three different cell morphologies: cells with normal lamellae, cells that spread but exhibited an abnormal serrated edge (Fig. 4 c), and cells exhibiting the stellate morphology observed after RNAi of Arp2/3 and SCAR (Fig. 4 d). The serrated cell shape likely represents an intermediate morphology caused by incomplete inhibition of the signaling pathway. In control RNAi-treated cells, >95% of the cells formed normal lamellae with <5% of the cells exhibiting a serrated cell margin (Table II). Stellate cells were never observed in control cultures. Inhibition of Nck alone by RNAi caused a reduction in the number of S2 cells with normal lamellae to ~65% and an increase in serrate cells to ~30% and stellate cells to 5% (Table II). Double RNAi treatments to inhibit Nck and Rac1/2 or Nck and Mtl produced moderate increases in the number of serrate cells compared with Nck alone. However, simultaneous application of dsRNAs against Nck, Rac1/2, and Mtl induced a dramatic increase in serrate and stellate cells to ~30 and ~20%, respectively. Our observations provide in vivo confirmation of the findings of Eden et al. (2002) and also suggest that the Rac-like proteins and Nck are partially redundant for lamella formation in S2 cells.

Discussion

We have developed a novel system for the study of actin cytoskeletal dynamics that is amenable to in vivo imaging and

The Journal of Cell Biology

targeted inhibition of proteins via RNAi. From a set of 90 proteins implicated in actin dynamics, we have found 13 proteins that contribute to normal lamellae formation and seven proteins that are involved in cytokinesis. However, we cannot rule out the involvement of other proteins from our tested list. As with all RNAi-mediated "knockdown" screens, negative results are not definitively conclusive without demonstrating that the actual target protein is depleted. Moreover, it also remains possible that a small amount of residual protein that remains after RNAi treatment is sufficient for cellular function. In addition, it is possible that some actin dynamics phenotypes may only become apparent by time-lapse microscopy. For example, perturbation of mammalian enabled/VASP did not cause gross changes in cellular morphology (Bear et al., 2002), as we have found for S2 cells, but drastically altered lamellae behavior and membrane ruffling. Time-lapse observation is very time consuming for the relatively large number of genes investigated in this study, however, we plan more detailed examination of actin dynamics by live cell microscopy for a smaller number of RNAi experiments in the future.

In this work, we found that a relatively small number of the proteins tested is essential for lamella protrusion. These proteins include: (a) an actin-nucleating factor (Arp2/3) and one of its activators (SCAR), (b) a factor that caps barbed ends of newly formed actin filaments (capping protein), (c) proteins involved in severing and depolymerizing actin filaments to allow turnover (cofilin and Aip1), and (d) factors that sequester actin monomers and promote nucleotide exchange (profilin and CAP). This set of proteins and observed RNAi phenotypes are consistent with current models for the cycle of actin dynamics in lamellae (Pollard et al., 2000; Pollard and Borisy, 2003). Moreover, these proteins are similar to the minimal set needed to reconstitute actin-based propulsion of *Listeria* in vitro (Loisel et al., 1999).

Although our results largely agree with the protein requirements for reconstitution of actin-based motility in vitro as described above, some observations reveal that actin dynamics in the cell are more complex. For example, two actin monomer–binding proteins (profilin and CAP) are required for normal lamella formation, whereas profilin alone is sufficient to facilitate movement in vitro, although the role of CAP has not yet been tested (Loisel et al., 1999). Our result indicates that these two proteins play distinct and nonredundant roles in cells, although loss of either yields a similar phenotype consisting of uniformly distributed actin filaments throughout the cytoplasm, as opposed to being confined to the leading edge, and a failure to spread. CAP was shown to bind actin monomers and inhibit polymerization in vitro (Gieselmann and Mann, 1992; Freeman et al., 1995) but has been less well studied biochemically than profilin. A careful side-by-side comparison of the effects of CAP and profilin on actin dynamics and nucleotide exchange may provide insight into why the cell needs both proteins to recycle actin for polymerization at the leading edge. In addition, we find that cells require the depolymerizing protein cofilin as well as the cofilin-interacting protein Aip1 to form lamella, whereas cofilin alone suffices in vitro (Loisel et al., 1999). Previous biochemical studies have suggested that Aip1 acts synergistically with cofilin to promote actin filament disassembly (Okada et al., 1999; Rodal et al., 1999), and this synergy may be essential for cofilin function in vivo. We have also observed a role for slingshot, a cofilin phosphatase, for normal lamellae morphology, further underscoring the role for actin disassembly for S2 cell spreading. A third unanticipated result was the partial defect in lamella organization in cytoplasmic myosin II RNAi cells. Cytoplasmic myosin II is generally believed to be important for the retraction of the trailing end of migrating cells (Eddy et al., 2000) and in generating the fan-shaped appearance of the lamella in migrating keratocytes (Pollard and Borisy, 2003). Our phenotype shows that myosin II plays a role in the organization of actin filaments in the lamella of nonmigrating cell types as well, although it is not essential for cell spreading.

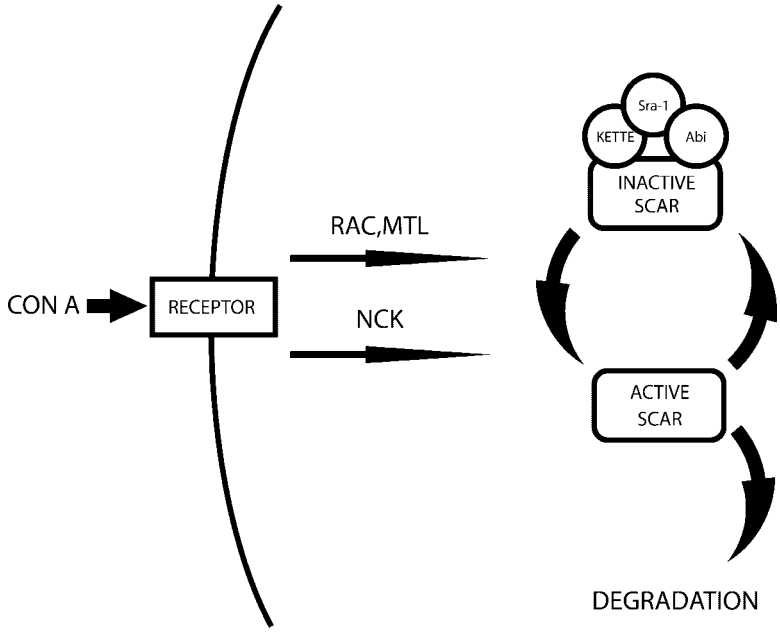

Figure 5. **Model for the signaling pathway leading to SCAR activation during S2 cell lamella formation.** The con A–coated coverslip activates both Rac proteins and Nck by initially cross-linking an unidentified cell surface receptor(s). The Rac proteins and Nck signal through parallel pathways to cause dissociation of trans-inhibited SCAR bound by a complex of kette, Sra-1, and Abi. After dissociation, SCAR is able to promote actin nucleation by Arp2/3 at the cell membrane. SCAR may then be inactivated either by reassociation with its inhibitory complex or by degradation.

The Journal of Cell Biology

Our studies also have provided new insight into the activation of SCAR, which is summarized in the model shown in Fig. 5. Plasma membrane receptors on S2 cells (currently unknown) are activated, perhaps by cross-linking upon contact with con A–treated coverslips. Subsequently, two parallel pathways transduce this stimulus. One is mediated by small GTPases belonging to the Rac family. Our results show that three Rac GTPases (Rac1, Rac2, and Mtl1) participate in the transduction pathway, confirming the functional redundancy of these proteins reported in many fly tissues (Hakeda-Suzuki et al., 2002). A second transduction pathway is mediated by the SH2-SH3 adaptor protein Nck, which has been shown to activate SCAR in vitro (Eden et al., 2002). Our results confirm that this Nck-mediated activation of SCAR is important in vivo as well. The Rac and SCAR pathways probably converge in activating actin polymerization by dissociating SCAR from its trans-inhibited kette–Sra-1–Abi-bound complex and allowing it to bind to Arp2/3 (Eden et al., 2002). Moreover, the finding that simultaneous inhibition of Rac-like proteins and Nck does not completely mimic SCAR RNAi treatment raises the possibility that additional SCAR activators exist.

Our work also has uncovered an additional role of the kette–Sra-1–Abi complex in protecting SCAR from degradation. Unlike the WASP protein, which is autoinhibited (Pollard and Borisy, 2003), SCAR is constitutively active (Machesky et al., 1999). Therefore, long-lived, uncomplexed SCAR may be detrimental, as it would cause uncontrolled actin polymerization. Thus, the degradation of free SCAR would ensure a proper stoichiometry of SCAR to its inhibitory complex. It is also possible that the kinetics of SCAR degradation may be regulated under some circumstances to modulate actin cytoskeleton dynamics. Further studies are underway to explore this potential avenue of SCAR regulation and understand the mechanism of SCAR degradation.

Given the relative ease and effectiveness of RNAi-mediated gene inhibition, we foresee that S2 and other *Drosophila* tissue culture cells can be used to explore other aspects of the actin cytoskeleton, such as filopodia formation. If proper cues are provided to these cells, cell migration and cell polarity may be amenable to investigation as well. Moreover, although we restricted our studies to known actin-binding proteins, genome-wide screens can be performed to identify novel genes associated with cytoskeletal regulation.

Materials and methods

Cell culture and double-stranded RNAi

Schneider S2 cells were grown and plated on con A as previously described (Rogers et al., 2002). In brief, RNAi was performed on S2 cells cultured in six-well tissue culture plates for 7 d according to the methods of Clemens et al. (2000) using PCR products flanked at their 5′ and 3′ ends by T7 sequences. Primers for target genes were designed using software written in-house in Perl. Individual primer sequences may be found in the online supplemental material (available at http://www.jcb.org/cgi/content/full/jcb.200303023/DC1). dsRNA was produced by in vitro transcription using Megascript kits (Ambion) according to the manufacturer's instructions. At the end of the 7-d treatment, cells were resuspended and plated on con A–treated coverslips, allowed to spread for ~1 h, and then processed for microscopy.

Antibodies

The following antibodies were used: goat anti-Arp2 (yN-16; Santa Cruz Biotechnology, Inc.); guinea pig anti–*Drosophila* SCAR (Zallen et al., 2002); rabbit anti–*Drosophila* capping protein β subunit and mouse anti–myosin VI (gifts of K. Miller, Washington University, St. Louis, MO); rabbit anti–*Drosophila* cofilin/twinstar (gift of T. Uemura, Kyoto University, Kyoto, Japan); anti-profilin/chickadee monoclonal (chi1J; Developmental Studies Hybridoma Bank) (Verheyen and Cooley, 1994); anti-enabled monoclonal (5G2; Developmental Studies Hybridoma Bank) (Bashaw et al., 2000); anti-fascin/singed monoclonal (sn7C; Developmental Studies Hybridoma Bank); anti-Rho1 (P1D9; Developmental Studies Hybridoma Bank); rabbit anti-diaphanous (gift of S. Wasserman, University of California, San Diego, CA); rabbit anti-Pod1 (gift of M. Rothenberg, University of California, San Francisco); rabbit anti-Dock (gift of C. Worby, University of California, San Diego, San Diego, CA); and rabbit anti-Trio (gift of B. Dickson, Research Institute of Molecular Pathology, Vienna, Austria).

Immunofluorescence microscopy

For staining of filamentous actin, S2 cells were rinsed in HL3 buffer (70 mM NaCl, 5 mM KCl, 1.5 mM $CaCl_2$-$2H_2O$, 20 mM $MgCl_2$-$6H_2O$, 10 mM $NaHCO_3$, 5 mM trehalose, 115 mM sucrose, 5 mM Hepes, pH 7.2) (Stewart et al., 1994) and fixed for 10 min with 10% paraformaldehyde (EM Sciences) in HL3 buffer. The cells were then permeabilized with 0.1% Triton X-100 in PBS (PBST) and stained with 165 nM Texas red-X phalloidin (Molecular Probes) and 0.5 μg/ml DAPI. For antibody staining, the cells were blocked in 5% normal goat serum in PBST and treated with primary antibodies in the same solution for 1 h. After washing, cells were stained with secondary antibodies (Cy2 goat anti–rabbit, donkey anti–mouse, or goat anti–guinea pig, all at a dilution of 1:300) (Jackson ImmunoResearch Laboratories). After washing in PBST, the cells were rinsed in distilled water and mounted under 90% glycerol/10% borate, pH 9.0, supplemented with 5% *N*-propyl gallate. Images were acquired with an Orca II cooled CCD camera (Hamamatsu) using a 100X/1.4 N.A objective lens mounted on a Nikon TE300 inverted microscope driven by Simple PCI software (Compix, Inc.). Grayscale images were combined and colorized using Adobe Photoshop®. Image morphology and quantitation was performed with ImageJ (http://rsb.info.nih.gov/ij/). Some images were enhanced using a no-neighbor deconvolution algorithm using Huygens Pro software (Scientific Volume Imaging).

Online supplemental material

The supplemental material (Videos 1–4 and Fig. S1; available at http://www.jcb.org/cgi/content/full/jcb.200303023/DC1) shows the behavior of the actin cytoskeleton in *Drosophila* S2 cells by time-lapse fluorescence microscopy. Culture of these cells on con A–coated glass induces the cells to attach, spread, and elaborate a lamellipodia. Observation of GFP–actin reveals that lamellae thus formed exhibit cycles of extension, retraction, and retrograde flow.

We are grateful to Mark Dayel, Dyche Mullins, and Jack Taunton for valuable discussion during this project. We also thank Dyche Mullins for the use of his microscope and Julie Hollien and Jonathan Weissman for sharing their unpublished results.

This work was supported by a National Institutes of Health postdoctoral training grant (5F32GM064966-02).

Submitted: 4 March 2003
Accepted: 28 July 2003

References

Ayscough, K.R., and D.G. Drubin. 1996. ACTIN: general principles from studies in yeast. *Annu. Rev. Cell Dev. Biol.* 12:129–160.

Bashaw, G.J., T. Kidd, D. Murray, T. Pawson, and C.S. Goodman. 2000. Repulsive axon guidance: Abelson and Enabled play opposing roles downstream of the Roundabout receptor. *Cell.* 101:703–715.

Baum, B., W. Li, and N. Perrimon. 2000. A cyclase-associated protein regulates actin and cell polarity during *Drosophila* oogenesis and in yeast. *Curr. Biol.* 10: 964–973.

Bear, J.E., T.M. Svitkina, M. Krause, D.A. Schafer, J.J. Loureiro, G.A. Strasser, I.V. Maly, O.Y. Chaga, J.A. Cooper, G.G. Borisy, and F.B. Gertler. 2002. Antagonism between Ena/VASP proteins and actin filament capping regulates fibroblast motility. *Cell.* 109:509–521.

Ben-Yaacov, S., R. Le Borgne, I. Abramson, F. Schweisguth, and E.D. Schejter.

2001. Wasp, the *Drosophila* Wiskott-Aldrich syndrome gene homologue, is required for cell fate decisions mediated by Notch signaling. *J. Cell Biol.* 152:1–13.

Benlali, A., I. Draskovic, D.J. Hazelett, and J.E. Treisman. 2000. act up controls actin polymerization to alter cell shape and restrict Hedgehog signaling in the *Drosophila* eye disc. *Cell.* 101:271–281.

Clemens, J.C., C.A. Worby, N. Simonson-Leff, M. Muda, T. Maehama, B.A. Hemmings, and J.E. Dixon. 2000. Use of double-stranded RNA interference in *Drosophila* cell lines to dissect signal transduction pathways. *Proc. Natl. Acad. Sci. USA.* 97:6499–6503.

Cooley, L., E. Verheyen, and K. Ayers. 1992. chickadee encodes a profilin required for intercellular cytoplasm transport during *Drosophila* oogenesis. *Cell.* 69: 173–184.

Cooper, J.A., and D.A. Schafer. 2000. Control of actin assembly and disassembly at filament ends. *Curr. Opin. Cell Biol.* 12:97–103.

Cramer, L.P. 1997. Molecular mechanism of actin-dependent retrograde flow in lamellipodia of motile cells. *Front. Biosci.* 2:d260–d270.

Eddy, R.J., L.M. Pierini, F. Matsumura, and F.R. Maxfield. 2000. Ca^{2+}-dependent myosin II activation is required for uropod retraction during neutrophil migration. *J. Cell Sci.* 113:1287–1298.

Eden, S., R. Rohatgi, A.V. Podtelejnikov, M. Mann, and M.W. Kirschner. 2002. Mechanism of regulation of WAVE1-induced actin nucleation by Rac1 and Nck. *Nature.* 418:790–793.

Etienne-Manneville, S., and A. Hall. 2002. Rho GTPases in cell biology. *Nature.* 420:629–635.

Freeman, N.L., Z. Chen, J. Horenstein, A. Weber, and J. Field. 1995. An actin monomer binding activity localizes to the carboxyl-terminal half of the *Saccharomyces cerevisiae* cyclase-associated protein. *J. Biol. Chem.* 270:5680–5685.

Gieselmann, R., and K. Mann. 1992. ASP-56, a new actin sequestering protein from pig platelets with homology to CAP, an adenylate cyclase-associated protein from yeast. *FEBS Lett.* 298:149–153.

Goshima, G., and R.D. Vale. 2003. The roles of microtubule-based motor proteins in mitosis: comprehensive RNAi analysis in the *Drosophila* S2 cell line. *J. Cell Biol.* 162:1003–1016.

Gournier, H., E.D. Goley, H. Niederstrasser, T. Trinh, and M.D. Welch. 2001. Reconstitution of human Arp2/3 complex reveals critical roles of individual subunits in complex structure and activity. *Mol. Cell.* 8:1041–1052.

Gunsalus, K.C., S. Bonaccorsi, E. Williams, F. Verni, M. Gatti, and M.L. Goldberg. 1995. Mutations in twinstar, a *Drosophila* gene encoding a cofilin/ADF homologue, result in defects in centrosome migration and cytokinesis. *J. Cell Biol.* 131:1243–1259.

Hakeda-Suzuki, S., J. Ng, J. Tzu, G. Dietzl, Y. Sun, M. Harms, T. Nardine, L. Luo, and B.J. Dickson. 2002. Rac function and regulation during *Drosophila* development. *Nature.* 416:438–442.

Holt, M.R., and A. Koffer. 2001. Cell motility: proline-rich proteins promote protrusions. *Trends Cell Biol.* 11:38–46.

Lauffenburger, D.A., and A.F. Horwitz. 1996. Cell migration: a physically integrated molecular process. *Cell.* 84:359–369.

Loisel, T.P., R. Boujemaa, D. Pantaloni, and M.F. Carlier. 1999. Reconstitution of actin-based motility of *Listeria* and Shigella using pure proteins. *Nature.* 401:613–616.

Machesky, L.M., R.D. Mullins, H.N. Higgs, D.A. Kaiser, L. Blanchoin, R.C. May, M.E. Hall, and T.D. Pollard. 1999. Scar, a WASp-related protein, activates nucleation of actin filaments by the Arp2/3 complex. *Proc. Natl. Acad. Sci. USA.* 96:3739–3744.

Mitchison, T.J., and L.P. Cramer. 1996. Actin-based cell motility and cell locomotion. *Cell.* 84:371–379.

Mogilner, A., and G. Oster. 1996. Cell motility driven by actin polymerization. *Biophys. J.* 71:3030–3045.

Montell, D.J. 1999. The genetics of cell migration in *Drosophila* melanogaster and *Caenorhabditis elegans* development. *Development.* 126:3035–3046.

Niwa, R., K. Nagata-Ohashi, M. Takeichi, K. Mizuno, and T. Uemura. 2002. Control of actin reorganization by Slingshot, a family of phosphatases that dephosphorylate ADF/cofilin. *Cell.* 108:233–246.

Okada, K., T. Obinata, and H. Abe. 1999. XAIP1: a *Xenopus* homologue of yeast actin interacting protein 1 (AIP1), which induces disassembly of actin filaments cooperatively with ADF/cofilin family proteins. *J. Cell Sci.* 112:1553–1565.

Pollard, T.D., and G.G. Borisy. 2003. Cellular motility driven by assembly and disassembly of actin filament. *Cell.* 112:453–465.

Pollard, T.D., L. Blanchoin, and R.D. Mullins. 2000. Molecular mechanisms controlling actin filament dynamics in nonmuscle cells. *Annu. Rev. Biophys. Biomol. Struct.* 29:545–576.

Rodal, A.A., J.W. Tetreault, P. Lappalainen, D.G. Drubin, and D.C. Amberg. 1999. Aip1p interacts with cofilin to disassemble actin filaments. *J. Cell Biol.* 145:1251–1264.

Rogers, S.L., G.C. Rogers, D.J. Sharp, and R.D. Vale. 2002. *Drosophila* EB1 is important for proper assembly, dynamics, and positioning of the mitotic spindle. *J. Cell Biol.* 158:873–884.

Small, J.V., T. Stradal, E. Vignal, and K. Rottner. 2002. The lamellipodium: where motility begins. *Trends Cell Biol.* 12:112–120.

Somma, M.P., B. Fasulo, G. Cenci, E. Cundari, and M. Gatti. 2002. Molecular dissection of cytokinesis by RNA interference in *Drosophila* cultured cells. *Mol. Biol. Cell.* 13:2448–2460.

Stewart, B.A., H.L. Atwood, J.J. Renger, J. Wang, and C.F. Wu. 1994. Improved stability of *Drosophila* larval neuromuscular preparations in haemolymph-like physiological solutions. *J. Comp. Physiol.* 175:179–191.

Verheyen, E.M., and L. Cooley. 1994. Profilin mutations disrupt multiple actin-dependent processes during *Drosophila* development. *Development.* 120: 717–728.

Waterman-Storer, C.M., A. Desai, J.C. Bulinski, and E.D. Salmon. 1998. Fluorescent speckle microscopy, a method to visualize the dynamics of protein assemblies in living cells. *Curr. Biol.* 8:1227–1230.

Welch, M.D., and R.D. Mullins. 2002. Cellular control of actin nucleation. *Annu. Rev. Cell Dev. Biol.* 18:247–288.

Zallen, J.A., Y. Cohen, A.M. Hudson, L. Cooley, E. Wieschaus, and E.D. Schejter. 2002. SCAR is a primary regulator of Arp2/3-dependent morphological events in *Drosophila*. *J. Cell Biol.* 156:689–701.